



Cite this: *New J. Chem.*, 2019, **43**, 17696

Received 3rd May 2019,
Accepted 4th July 2019

DOI: 10.1039/c9nj02275a

rs.c.li/njc

Vanadium(v) complexes of mandelic acid†

Filip Zechel,^a Peter Schwendt,^a Róbert Gyepes,^b Ján Šimunek,^a Jozef Tatiersky^a and Lukáš Krivosudský^{b,*ac}

New vanadium complexes of mandelic acid ($\text{NMe}_4)_4[\text{V}_2\text{O}_4((R)\text{-mand})_2][\text{V}_2\text{O}_4((S)\text{-mand})_2]$ (**1**), $(\text{NMe}_4)_2[\text{V}_2\text{O}_4((S)\text{-mand})_2]\cdot\text{H}_2\text{O}$ (**2**), $(\text{NEt}_4)_2[\text{V}_2\text{O}_4((S)\text{-mand})_2]\cdot\text{H}_2\text{O}$ (**3**), $(\text{PPh}_4)_2[\text{V}_2\text{O}_4((R)\text{-mand})((S)\text{-mand})]\cdot 2\text{H}_3\text{CCOCH}_3\cdot 2\text{H}_2\text{O}$ (**4**), and $(\text{NH}_4)_{2.5}(\text{NEt}_4)_{0.5}[\text{V}_3\text{O}_7((R)\text{-mand})((S)\text{-mand})]\cdot 2\text{H}_2\text{O}$ (**5**) (mand^{2-} = mandelato ligand) have been synthesized and characterized by single crystal X-ray diffraction and FT-IR spectroscopy. The band assignment in the IR spectra was corroborated by DFT calculations. While the structures of **1–4** comprise the expected dinuclear $[\text{V}_2\text{O}_4(\text{mand})_2]^{2-}$ (V_2L_2) anions, the structure of $[\text{V}_3\text{O}_7((R)\text{-mand})((S)\text{-mand})]^{3-}$ (V_3L_2) in **5** is unique and represents a new structural type in vanadium(v) chemistry. Solution studies of vanadate with mandelic acid by ^{51}V NMR revealed the presence of two dominant species V_2L_2 and V_3L_2 in aqueous solutions and increasing fraction of V_3L_2 species at slightly acidic pH (pH \approx 6).

Introduction

Vanadium participates in an essential way in several biochemical processes. This element was found at the active centre of some enzymes, including vanadium dependent nitrogenases or vanadium haloperoxidases which enable halogenation of organic compounds.¹ On the other hand α -hydroxycarboxylic acids are also involved in many basic biochemical processes (such as the Krebs cycle, Cori cycle, photorespiration and others).² Due to the importance of both vanadates and α -hydroxycarboxylic acids the mutual interaction of these groups of compounds was intensively studied.^{3–5} ^{51}V NMR studies revealed complex equilibria involving several species of different nuclearities; however, solid state investigations confirmed with certainty only dinuclear complexes.⁶ The dominant components in the vanadate- α -hydroxycarboxylic acid system, apart from common vanadates, are the dinuclear and trinuclear complexes of the composition V_2L_2 and V_3L_2 (L = anion of the α -hydroxycarboxylic acid) accompanied by a mononuclear complex VL .⁷ Several dinuclear vanadium(v) complexes with α -hydroxycarboxylato ligands were also reported in the solid state: $(\text{NH}_4)_2[\text{V}_2\text{O}_4(\text{glyc})_2]$,^{8,9} $\text{Rb}_2[\text{V}_2\text{O}_4(\text{glyc})_2]$,¹⁰ $\text{Na}_2[\text{V}_2\text{O}_4(\text{mlact})_2]\cdot 7\text{H}_2\text{O}$,¹¹ $(\text{NBu}_4)_2[\text{V}_2\text{O}_4(\text{mlact})_2]\cdot 2\text{H}_2\text{O}$,¹² $(\text{NH}_4)_2[\text{V}_2\text{O}_4(\text{ehba})_2]\cdot \text{H}_2\text{O}$,¹³

and $\text{Cs}_2[\text{V}_2\text{O}_4((S)\text{-lact})_2]\cdot 2\text{H}_2\text{O}$ ^{10,†} and a richer series of vanadium complexes with α -hydroxycarboxylic acids with more than one carboxyl group such as malic,¹⁴ citric,^{15–23} homocitric²⁴ and tartaric acid.^{25–28} The crystal structures confirmed the composition and geometry as were proposed by ^{51}V NMR spectroscopy; however, the V_3L_2 complexes do not have a model compound with a solved crystal structure. In this list, mandelato complexes are obviously missing. Mandelic acid is a common chiral aromatic α -hydroxycarboxylic acid (Scheme 1). Isolation of non-peroxido vanadium(v) complexes of mandelic acid was, so far, not possible mainly due to its strong reduction potential towards V^{V} . In this work we augment the family of vanadium(v) complexes of α -hydroxycarboxylic acids by mandelato complexes. We present the synthesis and characterization of dinuclear V_2L_2 complexes and a trinuclear V_3L_2 complex which revealed a surprising structure not identical to the previously proposed geometry.

Experimental

Materials and methods

All chemicals were of analytical grade and used as received. Stock aqueous solutions of $(\text{NMe}_4)\text{VO}_3$ and $(\text{NEt}_4)\text{VO}_3$ (1 mol dm^{-3}) were prepared by dissolution of V_2O_5 in conc. $(\text{NMe}_4)\text{OH}$ and $(\text{NEt}_4)\text{OH}$, adjustment of the pH to 8.0 and dilution. Elemental analyses (C, H, and N) were performed on a Vario MIKRO cube (Elementar). The analysis of hydrogen might be influenced by hygroscopic properties of the samples. Vanadium was determined gravimetrically as V_2O_5 . Solid state IR spectra were recorded on a Thermo Scientific Nicolet 6700 FT IR spectrometer in Nujol mulls,

^a Department of Inorganic Chemistry, Faculty of Natural Sciences, Comenius University in Bratislava, Mlynská dolina, Ilkovičova 6, 842 15 Bratislava, Slovakia

^b Department of Inorganic Chemistry, Faculty of Science, Charles University, Hlavova 2030, 128 00 Praha, Czech Republic

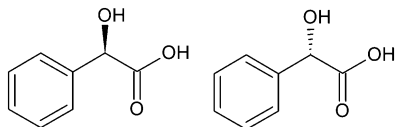
^c Universität Wien, Fakultät für Chemie, Institut für Biophysikalische Chemie, Althanstraße 14, Wien 1090, Austria. E-mail: lukas.krivosudsky@univie.ac.at

† Electronic supplementary information (ESI) available. CCDC 1911693–1911697.

For ESI and crystallographic data in CIF or other electronic format see DOI: 10.1039/c9nj02275a

‡ Abbreviations of ligands: glyc^{2-} – glycolato, lact^{2-} – lactato, mlact^{2-} – methyl-lactato, ehba^{2-} – 2-ethyl-2-hydroxybutanoato.





Scheme 1 Stereoisomers of mandelic acid (*R*)-(–)- $H_2mand = D-H_2mand$ and (*S*)-(–)- $H_2mand = L-H_2mand$.

KBr pellets and by the ATR technique. The ^{51}V NMR spectra were recorded at 278 K on a Varian Mercury Plus 600 MHz spectrometer operating at 157.88 MHz for ^{51}V in 5 mm tubes. Chemical shifts (δ) are given in ppm relative to $VOCl_3$ as an external standard ($\delta = 0$ ppm).

X-ray diffraction

Diffraction data were collected using a Kappa Apex II (Bruker) diffractometer equipped with a Cryostream Cooler (Oxford Cryosystems) and D8 VENTURE Kappa Duo (Bruker) using detector PHOTON 100 CMOS. Data were collected using graphite-monochromated Mo $K\alpha$ radiation ($\lambda = 0.71073$ Å) and were corrected for radiation absorption and polarization effects by methods incorporated in the diffractometer software. The phase problem was solved by direct methods (SHELXS)²⁹ and refined by full-matrix least-squares based on F^2 (SHELXL).³⁰ All non-hydrogen atoms were refined with no restraints and with anisotropic displacement parameters. Hydrogen atoms were included in idealized positions and refined as riding atoms. Graphics were obtained with DIAMOND.³¹ In the case of compound 5 we were forced to use SQUEEZE to expel cations and molecules of the solvent because of heavy disorder. We therefore present only the structure of the anionic component of the compound. Crystal structure data and refinement details are summarized in Table S1 (see ESI†).

Calculation of infrared spectra

The molecular structure of $[V_2O_4((S)-mand)_2]^{2-}$ from compound 2 has been optimized at the DFT level with the BP86 functional^{32,33} using tight convergence criteria and an ultrafine integration grid *in vacuo*. We have employed the all-electron Wachsters+f(14s11p6d3f)/[8s6p4d1f] basis set^{34,35} for the vanadium atom and the 6-31++G(d,p) basis set^{36,37} for the remaining atoms. Afterwards, harmonic vibrational frequencies were calculated. Quantum chemical calculations were performed using the Gaussian 09 Revision D.01 program³⁸ and for subsequent potential energy distribution (PED) analysis the VEDA4 program was utilized.³⁹

Syntheses

$(NMe_4)_4[V_2O_4((R)-mand)_2][V_2O_4((S)-mand)_2]$ (1). To 9.4 mL of acetone, 0.4 mL of aqueous *rac*- H_2mand (0.5 mol dm^{-3} ; 0.2 mmol) and 0.2 mL of NMe_4VO_3 (1 mol dm^{-3} ; 0.2 mmol) were added. The solution was kept at -20 °C. After three weeks, yellow needle-like crystals of 1 were isolated. Yield: 50 mg (40% based on V). Analytical data for $C_{24}H_{36}N_2O_{10}V_2$ in % (calc. %): C 46.05 (46.91), H 6.24 (5.91), N 4.58 (4.56), V 16.3 (16.6).

$(NMe_4)_2[V_2O_4((S)-mand)_2] \cdot H_2O$ (2). To 9.5 mL of acetone, 0.3 mL of aqueous (*S*)- H_2mand (0.5 mol dm^{-3} ; 0.15 mmol)

and 0.2 mL of NMe_4VO_3 (1 mol dm^{-3} ; 0.2 mmol) were added. The solution was kept at -20 °C. After six weeks, yellow needle-like crystals of 2 were isolated. Yield: 25 mg (20% based on V). Analytical data for $C_{24}H_{38}N_2O_{11}V_2$ in % (calc. %): C 45.10 (45.58), H 6.05 (6.06), N 4.59 (4.43).

$(NEt_4)_2[V_2O_4((S)-mand)_2] \cdot H_2O$ (3). To 100 mL of acetone, 5 mL of NEt_4VO_3 (1 mol dm^{-3} ; 5 mmol) and 5 mL of (*S*)- H_2mand (1 mol dm^{-3} in *EtOH*; 5 mmol) were added. The solution was kept at -20 °C. After one day, yellow plate-like crystals of 3 were isolated. Yield: 69 mg (20% based on V). Analytical data for $C_{32}H_{54}N_2O_{11}V_2$ in % (calc. %): C 50.49 (51.61), H 7.40 (7.31), N 3.73 (3.76).

$(PPh_4)_2[V_2O_4((R)-mand)((S)-mand)] \cdot 2H_3CCOCH_3 \cdot 2H_2O$ (4). To 9.4 mL of acetone, 0.4 mL of aqueous *rac*- H_2mand (0.5 mol dm^{-3} ; 0.2 mmol), 0.2 mL of NMe_4VO_3 (1 mol dm^{-3} ; 0.2 mmol) and 0.225 g of PPh_4Cl (0.6 mmol) were added. The solution was kept at -20 °C. After one month yellow needle-like crystals of 4 were isolated. Yield: 44 mg (17% based on V). Analytical data for $V_2P_2C_{70}H_{68}O_{14}$ in % (calc. %): C 63.77 (64.82), H 4.92 (5.28), V 8.5 (7.9).

$(NH_4)_{2.5}(NEt_4)_{0.5}[V_3O_7((R)-mand)((S)-mand)] \cdot 2H_2O$ (5). The pH of an aqueous solution of NEt_4VO_3 (1.5 mL, $c = 1$ mol dm^{-3} , 1.5 mmol) was adjusted to 9.0 with concentrated NH_3 . Afterwards, the solution was mixed with 1.2 mL of aqueous solution of *rac*- H_2mand (1.2 mmol; $c = 1$ mol dm^{-3}). To the obtained solution acetone (35 mL) was added. The resulting solution was allowed to crystallize at -20 °C. After 3 weeks light yellow crystals in the form of rectangular plates were isolated. Yield: 117 mg (11% based on V). Analytical data for $C_{20}H_{36}N_3O_{15}V_3$ in % (calc. %): C 33.35 (33.77), H 6.46 (5.10), N 6.02 (5.91), V 21.89 (21.48).

The $(NEt_4)_3[V_2O_4(mlact)_2VO_2(OH)_2]$ (type V_3L_2) complex was obtained in the mixture with $(NEt_4)_2[VO_2(mlact)_2]$ (type V_2L_2).⁷ Attempts to isolate the V_3L_2 complex in a form suitable for X-ray studies failed. The proposed structure of this complex we discussed in the text.

Results and discussion

Crystal structures

The prepared dinuclear mandelato complexes can be divided into two groups. For compounds 1–3 we observed that the central $\{V_2O_4\}$ unit binds always to the mandelato anion of the same configuration. Thus, racemic compound 1 contains both enantiomers $[V_2O_4((S)-mand)_2]^{2-}$ and $[V_2O_4((R)-mand)_2]^{2-}$ related in the crystal packing by the center of symmetry (Fig. 1), while compounds 2 and 3 contain only the $[V_2O_4((S)-mand)_2]^{2-}$ anion. The $[V_2O_4((R)-mand)((S)-mand)]^{2-}$ anion in 4 contains both enantiomers of the racemic mandelic acid (Fig. 2). Because of the C_i symmetry it is a *meso*-anion. It can be concluded from the stereochemical point of view that the formation of vanadium(v) mandelato complexes is not stereospecific, because it is possible to obtain the chiral anion (1) and the achiral compound in complex (4) starting from a racemic precursor of *rac*-mandelic acid. Table 1 summarizes geometrical data for the anions in all compounds. As confirmed by the calculation of τ parameters in



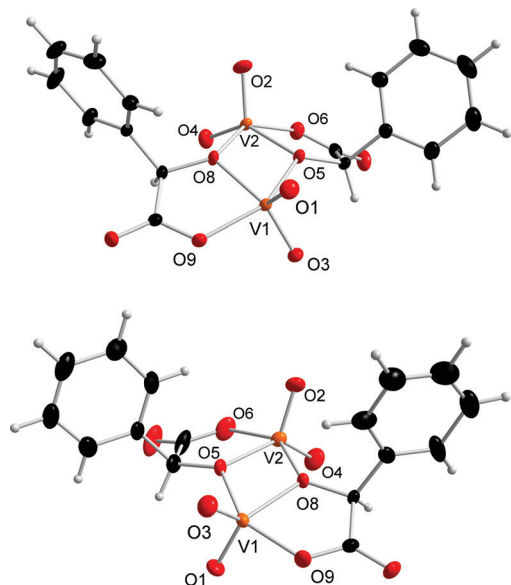


Fig. 1 Molecular structures of anions $[V_2O_4((R)\text{-mand})_2]^{2-}$ (upper, from **1**) and $[V_2O_4((S)\text{-mand})_2]^{2-}$ (lower, from **2**) showing atom labeling in the central $\{V_2O_8\}$ group. Colour code: V orange, O red, C black, and H grey. Displacement ellipsoids are displayed at a 30% probability level.

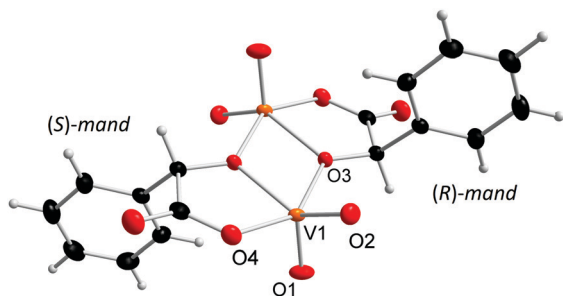


Fig. 2 Molecular structure of the anion $[V_2O_4((R)\text{-mand})((S)\text{-mand})]^{2-}$ found in compound **4** showing atom labeling in the central $\{V_2O_8\}$ group (symmetrically independent part). Colour code: V orange, O red, C black, and H grey. Displacement ellipsoids are displayed at a 30% probability level.

pentacoordinated systems, the vanadium atoms V1 and V2 form slightly distorted tetragonal pyramidal coordination geometry and are displaced above the calculated plane by about 0.5 Å. Axial positions are occupied by oxido ligands O1 and O2, respectively. The tetragonal pseudoplane is completed by one oxido ligand (O3, and O4, resp.), and one oxygen atom from the carboxylate anion (O6, and O9, resp.) and the two vanadium atoms are connected by hydroxylate oxygen atoms O5 and O8.

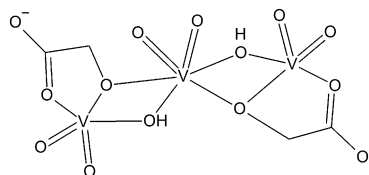
Compound **5** is the first isolated vanadium(v) complex of an α -hydroxycarboxylic with the stoichiometry V_3L_2 . Previous attempts to clarify the structure of such complexes relied mostly on ^{51}V NMR spectroscopy.⁷ The proposed structure is shown in Scheme 2. However, the X-ray structure analysis of **5** revealed a different structure (Fig. 3). The $[V_3O_7((R)\text{-mand})((S)\text{-mand})]^{3-}$ anion contains both enantiomers of *rac*-mandelic acid. Unlike in Scheme 2, all vanadium atoms are pentacoordinated. Two oxido ligands always occupy the axial positions and one equatorial

Table 1 Selected geometrical parameters of compounds **1–4**

Compound bond lengths and δ in Å					
		1	2	3	4*
V=O	V1–O1	1.6206(12)	1.621(4)	1.622(3)	1.6213(9)
	V2–O2	1.6213(13)	1.613(4)	1.617(3)	1.6248(8)
	V1–O3	1.6305(12)	1.617(4)	1.628(3)	—
	V2–O4	1.6308(13)	1.617(4)	1.636(3)	—
V–O _h	V1–O5	1.9730(10)	1.957(3)	1.954(3)	V1–O3' 1.9636(8)
	V2–O5	2.0438(11)	2.017(3)	2.033(3)	V1–O3 2.0319(8)
	V1–O8	2.0280(11)	2.015(3)	2.032(3)	1.9637(8)
	V2–O8	1.9690(11)	1.969(3)	1.980(3)	—
V–O _c	V1–O9	1.9714(11)	1.960(4)	1.965(3)	V1–O4 1.9775(9)
	V2–O6	1.9711(12)	1.989(4)	1.957(3)	—
τ_{V1}		0.2	0.38	0.11	0.15
δ_{V1}		0.527	0.533	0.487	0.513
τ_{V2}		0.04	0.15	0.18	—
δ_{V2}		0.565	0.555	0.533	—

O_h – oxygen atom from the original alcoholic group, O_c – oxygen atom from the original carboxylic acid group. τ – parameter calculated from two bond angles in the tetragonal pseudoplane as $(\alpha - \beta)/60$; $\tau = 0$ tetragonal pyramidal geometry, $\tau = 1$ trigonal bipyramidal geometry. δ – displacement of the V atom from the ideal plane calculated from the positions of four atoms forming the tetragonal pseudoplane. * – only symmetrically independent bond parameters of the anion are given.

position. The central vanadium atom V1 is further coordinated by two oxygen atoms coming from the hydroxylate group and the oxido ligand, O1. The oxygen atom, O1, represents an unexpected feature of the anion as it was not expected in V_3L_2 complexes. The bridging μ_3 -O1 ligand is connecting all three vanadium atoms of the anion. The coordination of the V2 atom is completed by the chelating mandelato ligand that coordinates through one hydroxylato (O2) and one carboxylate (O3) oxygen



Scheme 2 Structure of V_3L_2 type complexes as proposed by Tracey *et al.*⁷

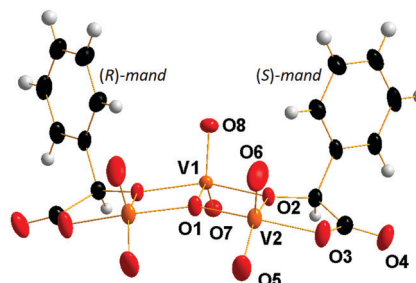


Fig. 3 Molecular structure of the anion $[V_3O_7((R)\text{-mand})((S)\text{-mand})]^{3-}$ found in **5** showing atom labeling in the central $\{V_3O_{12}\}$ group. Colour code: V orange, O red, C black, and H grey. Displacement ellipsoids are displayed at a 30% probability level.



Table 2 Selected geometrical parameters of compound **5**

Bond lengths and δ in Å*		
V=O	V2–O5	1.6157(17)
	V2–O6	1.6407(18)
	V1–O7	1.6419(18)
	V1–O8	1.6217(19)
V–O _h	V1–O2	1.9634(12)
	V2–O2	2.0183(13)
	V2–O3	1.9775(15)
V–O _c	V2–O1	1.9061(7)
V–(μ_3 -O)	V1–O1	1.9712(18)
Structural parameters		
Torsion angle (O8–V1...V2–O6)		23.930°
τ_{V1}		0.168
δ_{V1}		0.462
τ_{V2}		0.169
δ_{V2}		0.521

O_h – oxygen atom from the original alcoholic group, O_c – oxygen atom from the original carboxylic acid group. τ – parameter calculated from the two bond angles in the tetragonal pseudoplane as $(\alpha - \beta)/60$; $\tau = 0$ tetragonal pyramidal geometry, $\tau = 1$ trigonal bipyramidal geometry. δ – displacement of the V atom from the ideal plane calculated from the positions of four atoms forming the tetragonal pseudoplane.

atom. Key structural parameters of $[V_3O_7((R)\text{-mand})((S)\text{-mand})]^{3-}$ are summarized in Table 2.

The triangular center $[V_3(\mu_3\text{-O})]$ has been known in several vanadium(III, IV) complexes. However, most of these compounds exhibit D_{3h} symmetry; or at least approximate C_3 axis passing through the $(\mu_3\text{-O})$ atom.⁴⁰ In the case of anion $[V_3O_7((R)\text{-mand})((S)\text{-mand})]^{3-}$ the geometry around the O atom is different and it lies in the symmetry plane of the C_s symmetry.

In conclusion, the molecular structure of $[V_3O_7((R)\text{-mand})((S)\text{-mand})]^{3-}$ differs from the proposed one⁷ in: (1) the absence of bridging OH[−] groups between V1 and V2 atoms, (2) the presence of a bridging $(\mu_3\text{-O})$ ligand connecting all vanadium atoms, (3) the coordination number of the central vanadium atom; and (4) the overall symmetry C_s .

Infrared spectroscopy

The selected characteristic bands in the IR spectra of the prepared mandelato complexes and their assignment are summarized in Table 3 (the spectra are shown in Fig. S1–S10 (ESI[†]) and bands of the cations and solvents are tabulated in Table S2, (ESI[†])). All compounds exhibit typical strong bands corresponding to $\nu(\text{V=O})$ vibrations in the region around 930 cm^{−1} as well as to $\nu(\text{C–O})_h$, $\nu(\text{C–O})_{co}$ and $\nu(\text{C–O})_{un}$ (for symbols see Table 2) vibrations of the coordinated carboxylato ligand.

Theoretical calculations are very helpful for more precise band assignment using PED analysis that allows decomposing complicated vibrational movement of the molecule into several components. Thus, we employed this method for band assignment of the model $[V_2O_4((S)\text{-mand})_2]^{2-}$ anion from compound **2**. The theoretical values are in good agreement with experimental ones (Table 4) and enable reliable band assignment as shown in Table 3. We recently employed DFT calculations of IR spectra for several chiral and non-chiral vanadium(V) complexes using

Table 3 Selected bands in the IR spectra of the prepared compounds and their assignment

Characteristic group	Wavenumbers in cm ^{−1}				
	1	2	3	4	5
$\nu(\text{V=O})$	921 (s) 942 (s)	928 (vs)	935 (s)	925 (s) 936 (m)	910 (s) 924 (vs)
$\nu(\text{C–O})_h$	1048 (m)	1059 (s) 1084 (m)	1061 (m)	1063 (m)	1072 (m)
$\nu(\text{C–O})_{co}$	1315 (m) 1332 (m)	1323 (s)	1304 (m) 1329 (m)		1298 (s) 1308 (s)
$\nu(\text{C–O})_{un}$	1654 (vs)	1655 (vs)	1655 (v)	1651 (s)	1672 (vs)

(C–O)_{un} – uncoordinated (C–O) groups, (C–O)_{co} – coordinated (C–O) groups and (C–O)_h – deprotonated alcoholic groups.

similar basis sets and methods demonstrating that the interpretation of IR spectra of distinct geometries may be performed reliably using theoretical calculations.^{41–43}

Solution studies of vanadate with mandelic acid

The ⁵¹V NMR spectra have been measured for a number of nonperoxido vanadium(V) α -hydroxycarboxylato complexes.^{7,13,44–47} The only published data on nonperoxido vanadium(V) complexes with mandelic acid⁴⁴ supposed the existence of complexes, “a” of the $n(\text{V}):n(\text{L}) = 1:1$ type with a signal at −532 ppm and, “b” with unknown stoichiometry, the signal for which appeared at −548 ppm. Studied α -hydroxycarboxylic acids can be divided into two groups: The first one consists of the α -hydroxycarboxylic acids containing one carboxylic acid group and one alcoholic group, e.g. glycolic, lactic and mandelic acids. The second group involves α -hydroxycarboxylic acids with more than one carboxyl and hydroxyl groups; such as citric,⁴⁵ glyceric or malic acids.⁴⁴ Accordingly, the anions of α -hydroxycarboxylic acids of the second group can act as flexi-dentate ligands and have greater protonation variability in complexes. The most thorough studies^{7,46} devoted to α -hydroxycarboxylic acids of the first group suggested the existence of two dominant complexes with $V_2L_2^{2-}$ and $V_3L_2^{3-}$ stoichiometries (L represents the α -hydroxycarboxylato-(2−) ligand). While the $V_2L_2^{2-}$ complex gives rise to one ⁵¹V NMR signal, the trinuclear complex exhibits different peaks for the central and “peripheral” vanadium atoms. Besides the signals of $V_2L_2^{2-}$ and $V_3L_2^{3-}$, very weak signals of other species (VL^- , VL^{2-} , VL^{3-} , and $V_4L_2^{4-}$) have also been observed. The ⁵¹V NMR investigation we performed in the $H_2VO_4^-/rac\text{-H}_2\text{mand}/H^+$ system agrees with the general picture of the composition of complexes obtained by Tracey *et al.*^{7,47} and Pettersson *et al.*⁴⁶ Summarized data from so far studied systems are given in Table 5.

In the ⁵¹V NMR spectrum of the $NMe_4VO_3\text{-}rac\text{-H}_2\text{mand-H}_2O$ system (Fig. 4), it is possible to identify two groups of species. Besides various vanadates (V_1 : $H_2VO_4^-$, V_2 : $H_2V_2O_7^{2-}$, V_4 : $V_4O_{12}^{4-}$, V_5 : $V_5O_{15}^{5-}$, and V_{10} : $H_xV_{10}O_{28}^{(6-x)-}$),⁴⁸ two broader peaks are present. The signal at −533 ppm corresponds mainly to the $V_2L_2^{2-}$ complex and the signal at −551 ppm arises from the central vanadium atom of the $V_3L_2^{3-}$ complex. The common signal of the two peripheral vanadium atoms of the $V_3L_2^{3-}$ complex is evidently overlapped by the signal at −533 ppm. This overlapped signal is sometimes observed as a downfield



Table 4 Selected infrared bands for $[V_2O_4((S)\text{-mand})_2]^{2-}$

Calculated wavenumbers with rel. intensity in parentheses	Experimental wavenumbers	Band assignment with PED
3096 (9)	2962 m	$\nu(\text{C-H})_{\text{ar}}$ 92%
3080 (11)	2888 m	$\nu(\text{C-H})_{\text{ar}}$ 92%
1653 (9)		$\nu(\text{C=O})_{\text{un}}$ 83%
1651 (100)	1659 vs	$\nu(\text{C=O})_{\text{un}}$ 83%
1299 (12)	1336 m-s	$\delta(\text{HCC})_{\text{ar}}$ 64%
1293 (52)	1323 s	$\nu(\text{C=O})_{\text{co}}$ 66%
1082 (11)	1084 m	$\nu(\text{C-O})_{\text{h}}$ 37% $\delta(\text{HCC})_{\text{ar}}$ 21%
1051 (15)	1059 s	$\nu(\text{C-O})_{\text{h}}$ 37% $\delta(\text{HCC})_{\text{ar}}$ 21%
968 (17), 964 (10), 953 (16), 951 (21)	928 vs	$\nu(\text{V=O})$ 91% (mean)
768 (8)	765 s	$\delta(\text{OCO})$ 26%
705 (11)	696 m	$\text{tors}(\text{HCCC})_{\text{ar}}$ 36%, $\text{tors}(\text{CCCC})_{\text{ar}}$ 18%
675 (5)	622 w	$\text{tors}(\text{HCCC})_{\text{ar}}$ 44%, $\text{tors}(\text{CCCC})_{\text{ar}}$ 39%
556 (6)	537 w	$\delta(\text{OC}_h\text{C}_c)_{\text{ar}}$ 23%, $\nu(\text{C}_c\text{-C}_h)$ 12%
420 (15)	444 s	$\delta(\text{OC}_h\text{C}_c)_{\text{ar}}$ 18%

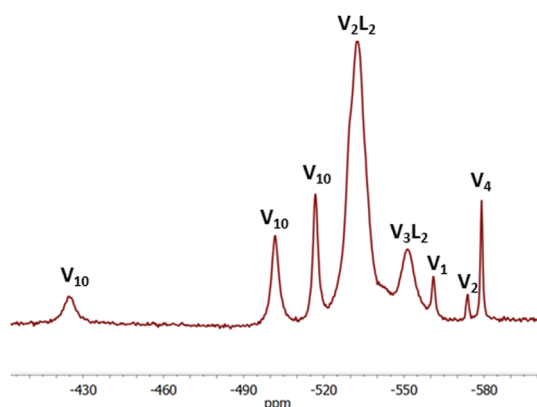
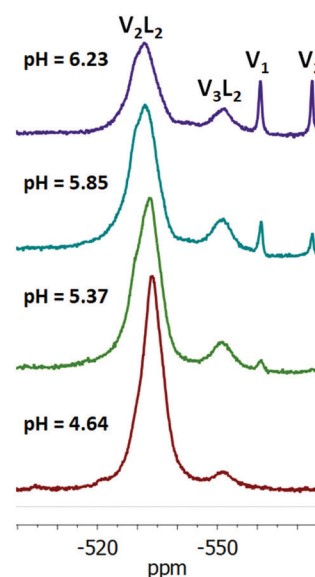
Relative intensities are given on the scale of 0–100, the bands with intensities < 5 were not included. ar – aromatic circle, un – uncoordinated C=O group, co – coordinated C–O group, C_c – carbon atom from the carboxylic acid group, C_h – carbon atom from the original alcoholic group.

Table 5 ^{51}V NMR chemical shifts of α -hydroxycarboxylato vanadium(v) complexes in aqueous solutions, and ionic strength 1.0 mol dm $^{-3}$ NaCl. Chemical shifts are given in ppm

	$V_3L_2^{3-}$			
	$V_2L_2^{2-}$	Central V	Peripheral V	Ref.
L-Lactic acid	–533	–550	–533	7
L-Lactic acid ^a	–533	–551	–532	46
α -Hydroxyisobutyric acid	–549	–569	–538	7
2-Ethyl-2-hydroxybutyric acid	–554	–578	–538	7
rac-Mandelic acid ^b	–533	–551	~–530	This work

^a Ionic strength of 0.15 mol dm $^{-3}$ NaCl. ^b Without adjustment of the ionic strength.

shoulder of the –533 ppm signal (Fig. 4). After subtraction of the doubled intensity of the –551 signal from the intensity of the –533 ppm signal, we can estimate the ratio of concentrations of the $V_2L_2^{2-}$ and $V_3L_2^{3-}$ complexes. This ratio decreases from pH = 4.65 (4.1) through pH = 5.37 (2.3), pH = 5.85 (1.4) and pH = 6.23 (1.2). Thus, the $V_3L_2^{3-}$ complex is supported by higher pH values (≈ 6) in agreement with the literature data (Fig. 5).^{7,46,47}

**Fig. 4** The ^{51}V NMR spectrum of the $\text{NMe}_4\text{VO}_3\text{-rac-H}_2\text{mand-H}_2\text{O}$ system, $c(\text{V}) = 0.03 \text{ mol dm}^{-3}$, $c(\text{rac-H}_2\text{mand}) = 0.02 \text{ mol dm}^{-3}$, pH = 5.72. Assignment of the chemical shifts: V_2L_2 –533 ppm, V_3L_2 –551 ppm, V_1 –561 ppm, V_2 –574 ppm, V_4 –579 ppm, and V_{10} –517 ppm, –502 ppm and –425 ppm.**Fig. 5** The ^{51}V NMR spectra of the $\text{NMe}_4\text{VO}_3\text{-NMe}_4\text{OH-rac-H}_2\text{mand-H}_2\text{O}$ system. $c(\text{V}) = 0.02 \text{ mol dm}^{-3}$, and $c(\text{rac-H}_2\text{mand}) = 0.02 \text{ mol dm}^{-3}$. The assignment of chemical shifts: V_2L_2 –534 ppm (pH = 4.64), –533 ppm (pH = 5.37), and –532 ppm (pH = 5.85 and 6.23); V_3L_2 –551 ppm (pH = 5.37); V_1 –561 ppm (pH = 5.37, 5.85 and 6.23); and V_2 –573 ppm (pH = 5.85 and 6.23).

As the complexes were isolated from mixed acetone–H $_2$ O solutions, we looked at the speciation also in mixed solvents (Fig. S11, ESI †). The addition of acetone to the aqueous solution results in the broadening of the peaks, raising the value of chemical shift and coalescence of the –551 ppm peak with the –533 ppm peak. On the other hand, the addition of acetone was necessary for the isolation of solid compounds from the solution.

Conclusions

In spite of the fact that the aqueous mandelic acid–vanadate system is prone to redox reactions, we succeeded in the synthesis of new vanadium(v) mandelato complexes by crystallization at



–20 °C in acetone–water solvent. Dinuclear chiral $[V_2O_4(mand)_2]^{2-}$ (V_2L_2) complexes in **1**, **2** and **3** contain only one enantiomer of the mandelate anion regardless of whether chiral or racemic mandelic acid was used in the synthesis. On the other hand, the dinuclear achiral $[V_2O_4((R)\text{-}mand)((S)\text{-}mand)]^{2-}$ anion in **4** comprises both enantiomers of the mandelato ligand. The $[V_3O_7((R)\text{-}mand)((S)\text{-}mand)]$ (V_3L_2) anion in **5** possesses several unique structural features. To the best of our knowledge, it is the first vanadium(v) trinuclear complex with a triangular $\{V_3-\mu_3O\}$ centre. The symmetry of the anion is C_S and it contains both enantiomers of mandelate. The solution studies confirmed the expected similarity of the mandelic acid–vanadate system in acid aqueous solutions to systems with other α -hydroxycarboxylic acids.

Conflicts of interest

There are no conflicts to declare.

Acknowledgements

This work was supported by the Scientific Grant Agency of the Ministry of Education of Slovak Republic and Slovak Academy of Sciences VEGA project no. 1/0507/17, and by the Slovak Research and Development Agency (APVV-17-0324). LK acknowledges financial support from the Austrian Science Fund (FWF), project no. M2200; and the University of Vienna. RG acknowledges support from Charles University Centre of Advanced Materials (CUCAM) (OP VVV Excellent Research Teams) CZ.02.1.01/0.0/0.0/15_003/0000417.

Notes and references

- 1 D. Rehder, *Bioinorganic vanadium chemistry*, Wiley, 2007.
- 2 P. Schwendt, P. Švančárek, I. Smatanová and J. Marek, *J. Inorg. Biochem.*, 2000, **80**, 59.
- 3 E. Bermejo, R. Carballo, A. Castiñeiras and A. B. Lago, *Coord. Chem. Rev.*, 2013, **257**, 2639.
- 4 W. T. Jin, W. Z. Wenig and Z. H. Zhou, *Eur. J. Inorg. Chem.*, 2019, 1228.
- 5 P. Schwendt, J. Tatiersky, L. Krivosudský and M. Šimuneková, *Coord. Chem. Rev.*, 2016, **318**, 135.
- 6 A. S. Tracey, G. R. Willsky and E. S. Takeuchi, *Vanadium. Chemistry, Biochemistry, Pharmacology and Practical Applications*, Taylor & Francis Group, 2007.
- 7 S. Hati, R. J. Batchelor, F. W. B. Einstein and A. S. Tracey, *Inorg. Chem.*, 2001, **40**, 6258.
- 8 Z. H. Zhou, J. Z. Wang, H. L. Wan and K. R. Tsai, *Chem. Res. Chin. Univ.*, 1994, **10**, 102.
- 9 S. Z. Hu, *Jiegou Huaxue*, 2000, **19**, 157.
- 10 M. Biagioli, L. Strinna-Erre, G. Micera, A. Panzanelli and M. Zema, *Inorg. Chim. Acta*, 2000, **310**, 1.
- 11 S. A. Bourne, J. J. Cruywagen and A. Kleinhorst, *Acta Crystallogr.*, 1999, **C55**, 2002.
- 12 I. Smatanová, J. Marek, P. Švančárek and P. Schwendt, *Acta Crystallogr.*, 1998, **C54**, 1249.
- 13 T. W. Hambley, R. J. Judd and P. A. Lay, *Inorg. Chem.*, 1992, **31**, 343.
- 14 M. Biagioli, L. Strinna-Erre, G. Micera, A. Panzanelli and M. Zema, *Inorg. Chim. Acta*, 2000, **310**, 1.
- 15 C. Gabriel, J. Venetis, M. Kaliva, C. P. Raptopoulou, A. Terzis, C. Drouza, B. Meier, G. Voyiatzis, C. Potamitis and A. Salifoglou, *J. Inorg. Biochem.*, 2009, **103**, 503.
- 16 M. Kaliva, C. P. Raptopoulou, A. Terzis and A. Salifoglou, *J. Inorg. Biochem.*, 2003, **93**, 161.
- 17 Z.-H. Zhou, H.-L. Wan, S.-Z. Hu and K.-R. Tsai, *Inorg. Chim. Acta*, 1995, **237**, 193.
- 18 M. Tsaramyrsi, D. Kavousanaki, C. P. Raptopoulou, A. Terzis and A. Salifoglou, *Inorg. Chim. Acta*, 2001, **320**, 47.
- 19 Z.-H. Zhou, W.-B. Yan, H.-L. Wan, K.-R. Tsai, J.-Z. Wang and S.-Z. Hu, *J. Chem. Crystallogr.*, 1995, **25**, 807.
- 20 D. W. Wright, P. A. Humiston, W. H. Orme-Johnson and W. M. Davis, *Inorg. Chem.*, 1995, **34**, 4194.
- 21 Z.-H. Zhou, H. Zhang, Y.-Q. Jiang, D.-H. Lin, H.-L. Wan and K.-R. Tsai, *Transition Met. Chem.*, 1999, **24**, 605.
- 22 C.-Y. Chen, Z.-H. Zhou, S.-Y. Mao and H.-L. Wan, *J. Coord. Chem.*, 2007, **60**, 1419.
- 23 M. Kaliva, T. Giannadaki, A. Salifoglou, C. P. Raptopoulou and A. Terzis, *Inorg. Chem.*, 2002, **41**, 3850.
- 24 D. W. Wright, R. T. Chang, S. K. Mandal, W. H. Armstrong and W. H. Orme-Johnson, *J. Biol. Inorg. Chem.*, 1996, **1**, 143.
- 25 J. Gálíková, P. Schwendt, J. Tatiersky, A. S. Tracey and Z. Žák, *Inorg. Chem.*, 2009, **48**, 8423.
- 26 P. Schwendt, A. S. Tracey, J. Tatiersky, J. Gálíková and Z. Žák, *Inorg. Chem.*, 2007, **46**, 3971.
- 27 P. Antal, P. Schwendt, J. Tatiersky, R. Gyepes and M. Drábik, *Transition Met. Chem.*, 2014, **39**, 893.
- 28 J. Cao, Y. Xiong, X. Luo, L. Chen, J. Shi, M. Zhou and Y. Xu, *Dalton Trans.*, 2018, **47**, 6054.
- 29 G. M. Sheldrick, *Acta Crystallogr.*, 2008, **A64**, 112.
- 30 G. M. Sheldrick, *Acta Crystallogr.*, 2015, **C71**, 3.
- 31 Diamond - Crystal and Molecular Structure Visualization. Crystal Impact - Dr H. Putz & Dr K. Brandenburg GbR, Kreuzherrenstr. 102, 53227 Bonn, Germany. <http://www.crystalimpact.com/diamond>.
- 32 A. D. Becke, *Phys. Rev.*, 1988, **A38**, 3098.
- 33 J. P. Perdew, *Phys. Rev.*, 1986, **B33**, 8822.
- 34 A. J. H. Wachters, *J. Chem. Phys.*, 1970, **52**, 1033.
- 35 C. W. Bauschlicher, S. R. Langhoff and L. A. Barnes, *J. Chem. Phys.*, 1989, **91**, 2399.
- 36 P. C. Hariharan and J. A. Pople, *Theor. Chim. Acta*, 1973, **28**, 213.
- 37 W. J. Hehre, R. Ditchfield and J. A. Pople, *J. Chem. Phys.*, 1972, **56**, 2257.
- 38 M. J. Frisch, G. W. Trucks, H. B. Schlegel, *et al.*, *Gaussian 09, Revision D.01*, Gaussian, Inc., Wallingford CT, 2013.
- 39 M. H. Jamroz, *Vibrational Energy Distribution Analysis VEDA 4*, Warsaw, 2004–2010.
- 40 M. R. Maurya, *Coord. Chem. Rev.*, 2019, **383**, 43.
- 41 G. Orešková, J. Chrappová, J. Puškelová, J. Šimunek, P. Schwendt, J. Noga and R. Gyepes, *Struct. Chem.*, 2016, **27**, 605.
- 42 L. Krivosudský, P. Schwendt, J. Šimunek and R. Gyepes, *J. Inorg. Biochem.*, 2015, **147**, 65.



- 43 L. Krivosudský, P. Schwendt, R. Gyepes and J. Šimunek, *Inorg. Chem. Commun.*, 2015, **56**, 105.
- 44 M. M. Caldeira, M. L. Ramos, N. C. Oliveira and V. M. S. Gil, *Can. J. Chem.*, 1987, **65**, 2434.
- 45 A. Gorzsás, K. Getty, I. Andersson and L. Petterson, *Dalton Trans.*, 2004, 2873.
- 46 A. Gorzsás, I. Andersson and L. Petterson, *Dalton Trans.*, 2003, 2503.
- 47 A. S. Tracey, *Coord. Chem. Rev.*, 2003, **237**, 113.
- 48 D. C. Crans and A. S. Tracey, *The Chemistry of Vanadium in Aqueous and Nonaqueous Solution*, ACS Symposium series, 1998, vol. 711, p. 2.

